

Proceedings Article

# Investigating methods for temperature reconstruction based on simulated data

Tobias Klemme<sup>a,\*</sup> · Thorsten M. Buzug<sup>a,b</sup> · Alexander Neumann<sup>a</sup>

<sup>a</sup>Institute of Medical Engineering, Universität zu Lübeck, Lübeck, Germany

<sup>b</sup>Fraunhofer Research Institution for Individualized and Cellbased Medical Engineering IMTE, Lübeck, Germany

\*Corresponding author, email: [klemme@imt.uni-luebeck.de](mailto:klemme@imt.uni-luebeck.de)

© 2022 Klemme *et al.*; licensee Infinite Science Publishing GmbH

This is an Open Access article distributed under the terms of the Creative Commons Attribution License (<http://creativecommons.org/licenses/by/4.0>), which permits unrestricted use, distribution, and reproduction in any medium, provided the original work is properly cited.

## Abstract

Magnetic particle imaging (MPI) leverages the nonlinear response of magnetic particles for imaging. Since the response of the particles is dependent on environmental parameters like temperature or viscosity it can reconstruct images of these properties. It has been shown that MPI is a promising tool to monitor temperatures using a reconstruction approach called multi-color MPI, which enables temperature imaging in applications such as magnetic particle hyperthermia. This work investigates different approaches to reconstruct temperature differences as well as different reconstruction schemes for multi-color MPI. The performed reconstructions are based on simulated 2D system matrices providing a reliable baseline for comparisons. The simulated system matrices are obtained by simulations of the magnetic particles in different magnetic offset fields corresponding to the spatial positions in a gradient field.

## I. Introduction

Imaging temperatures *in vivo* can be a useful tool to control temperatures in applications like magnetic fluid/particle hyperthermia (MFH/MPH) [1,2] or high-intensity focused ultrasound (HIFU) [3] and to assure the therapy goals of those applications. One imaging methodology capable to obtain images with temperature information is MPI since the particles used as tracer have a temperature dependent response. Precise temperature control requires a temperature resolution in the range below 1 K [4] since hyperthermia and the ablation of tumours require precise temperatures to ensure the destruction of the tumour, while the healthy tissue remains unaffected. Resolving temperatures in magnetic particle imaging (MPI) is possible [5,6,7] but a quantitative measurement of reproduceable temperature resolution is missing. This work compares different methods to obtain temperature differences from magnetic particle imaging as well as different reconstruction schemes.

Since the data for the reconstruction is acquired using simulations of the magnetic particles it can be assured that the difference between two signals at different temperatures is only affected by white noise and the given temperature difference. No experimental influences degrade the signal. Therefore, using data from simulations ensures a reliable baseline for comparisons.

## II. Material and methods

Measurements and 2D system matrices are obtained using a simulation introduced by Neumann *et al.* [8]. The code for the simulation is available in [9]. It is based on solving the coupled Langevin equations for the mechanical rotation and magnetization dynamics. Within this work, the particles are excited using a Lissajous sequence with a field amplitude of 12 mT and excitation frequencies of  $f_x = 24.5098$  kHz and  $f_y = 26.041$  kHz.

System matrices and phantoms are acquired by ap-

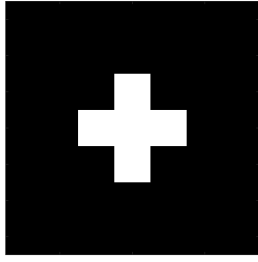


**Figure 1:** Simulated phantom for the reconstructions

plying offset fields corresponding to the spatial positions in a gradient field or voxel, respectively. The offset fields are set uniformly in a range from -16 mT to 16 mT for the x and y direction, where the discretization is chosen to be a 7x7 grid. The simulated particles have a core diameter of 25 nm and a hydrodynamic diameter of 50 nm. The surrounding fluid is assumed to have a viscosity of 1 mPa s (water). Further, the saturation magnetization and uniaxial anisotropy constant are set to 477464 A/m (Magnetite) and 4000 kJ/m<sup>3</sup>, respectively. The value of the anisotropy constant is chosen since [10] as shown that these values give the highest signals.

The total simulation time covers 3 periods of the Lissajous-trajectory ( $\approx 2$  ms) with a simulation timestep of 5 ps. To reduce the amount of data and noise, these timesteps are oversampled to a final timestep of 2  $\mu$ s (block averaged; not moving). To avoid initialization artefacts of the simulation, only the last two periods are used for the reconstruction. Each voxel is simulated with 10000 particles. Two system matrices have been simulated at temperatures of 295 K and 335 K. Additionally, four phantoms at 295 K, 315 K, 335 K and 355 K are also simulated. An image of the phantom is shown in Fig. 1. The spectral data is obtained by a Fourier-transform of the temporal derivative of the particle signal  $m(t)$  representing the induced signal  $u(t)$ .

### III. Results and discussion

For the reconstructions within this work only frequencies in the range from 75 kHz to 750 kHz with a signal to noise ratio exceeding 4 are considered, resulting in a total of 700 frequency components. Being able to reconstruct temperature differences in MPI relies on the fact that the magnetic response of the particles is temperature dependent. For simplicity, this temperature dependency is assumed to be linear. Commonly used particles experience an increase of amplitude with increasing temperatures [11]. However, this correlation depends on the physical properties of the particles and is mainly determined by the particle anisotropic energy  $K_u V_M$  and the Brownian relaxation, where  $K_u$  is the anisotropy constant and  $V_M$

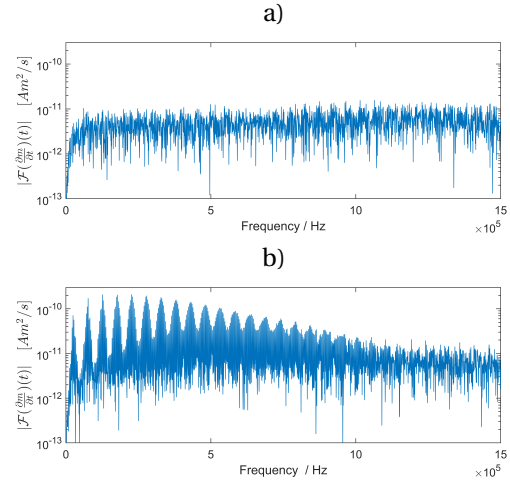


**Figure 2:** a) difference spectrum (x-channel)  $|U_{295K,1}(4,4)(\nu) - U_{295K,2}(4,4)(\nu)|$  b) difference spectrum  $|U_{335K}(4,4)(\nu) - U_{295K}(4,4)(\nu)|$

the core volume of the particle. The particle properties chosen within this work exhibit a decrease of spectral amplitude with increasing temperature. The reconstructions are performed using the Kaczmarz method (Kaz) as well as the iterative conjugate normal residual (CGNR) method applied on a regularized least square minimization problem.

#### III.I. Evaluation of simulation data

Fig. 2a shows the difference of the spectrums (x-channel) of two simulations at the same temperature (295K) at the middle voxel position (4,4). Only clean white noise is visible within the spectrum, which is expected and required to compare different reconstruction approaches without experimental uncertainty. Fig. 2b shows the difference of the amplitude spectrums between two simulations at voxel (4,4) at 295 K and 335 K resulting from  $|U_{335K}(4,4)(\nu) - U_{295K}(4,4)(\nu)|$ , where  $U_T(x, y)(\nu)$  represents the signal spectrum at location x, y at a temperature  $T$  and frequency  $\nu$ . The figure shows a significant difference in harmonics of the spectra at two different temperatures, indicating the possibility of temperature reconstruction using the simulations.

#### III.II. Multi-color approach

One approach to reconstruct the temperature differences is using the multi-color MPI approach [2] with concatenated system matrices given by  $S_{multi} = [S_{295K}, S_{335K}]$ . Resulting in the equation

$$\begin{bmatrix} S_{295K} & S_{335K} \end{bmatrix} \begin{bmatrix} \mathbf{c}_{T_1} \\ \mathbf{c}_{T_2} \end{bmatrix} = \mathbf{U}_T, \quad (1)$$

where  $S_{295K}$  and  $S_{335K}$  are the system matrices simulated at 295 K and 335 K respectively.  $\mathbf{c}_{T_1}$  and  $\mathbf{c}_{T_2}$  are the re-

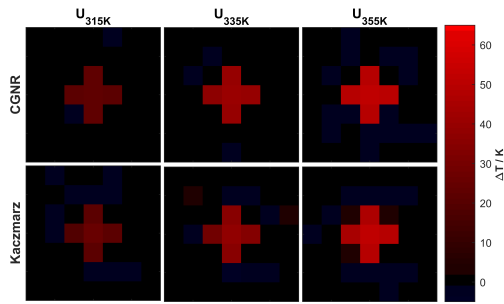


**Figure 3:** top: Multi color reconstruction using CGNR, bottom: multi-color reconstruction using Kaczmarz

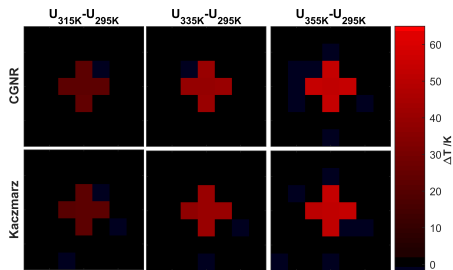


**Figure 4:** top: reconstruction using CGNR, bottom: reconstruction using the Kaczmarz method

constructed concentration at  $T_1$  and  $T_2$  and  $\mathbf{U}_T$  is the spectrum of the simulated particles at a temperature  $T$ .

The relative temperature difference is given by

$$\Delta T_{\text{rel}} \approx \frac{\mathbf{c}_{T_2}(x, y) - \mathbf{c}_{T_1}(x, y)}{\mathbf{c}_{T_1}(x, y) + \mathbf{c}_{T_2}(x, y)}, \quad (2)$$

where  $\Delta T_{\text{rel}}$  is the relative temperature difference to an intermediate temperature between 295 K and 335 K, which we assume to be 315 K. The  $\Delta T$  given within this paper will be calculated relative to a base temperature of 295 K, so that  $\Delta T = \Delta T_{\text{rel}} + 20\text{K}$ .

As already mentioned, this approach assumes that the particle signal is linearly proportional to the temperature. Fig. 3 shows the reconstructed images for the temperature differences with respect to the one at 295 K using the multi-color approach at the different temperatures (315 K, 335 K, 355 K). Two different reconstruction schemes are applied, using the Kaczmarz method Fig 3 bottom as well as CGNR Fig 3 top [12]. The regularization parameter  $\lambda$  is set to 0.0001 for CGNR and Kaz, while the number of iterations is set to 50 and 5, respectively. Tab.

**Table 1:** Temperature difference and deviation within the phantoms in Fig.3

$\mathbf{U}_T$	CGNR / $\approx \Delta T$	Kaczmarz / $\approx \Delta T$
$U_{315K}$	22.5 K $\pm$ 0.3 K	21.3 K $\pm$ 2.3 K
$U_{335K}$	39.1 K $\pm$ 1.3 K	34.6 $\pm$ 3.3 K
$U_{355K}$	50.1 $\pm$ 1.5 K	48.6 K $\pm$ 2.7 K

**Table 2:** Temperature difference and deviation within the phantoms in Fig.4

$\mathbf{U}_{\text{diff}}$	CGNR / $\Delta T$	Kaczmarz / $\Delta T$
$U_{315K} - U_{295K}$	22.4 K $\pm$ 0.4 K	22.2 K $\pm$ 0.76 K
$U_{335K} - U_{295K}$	40.5 K $\pm$ 0.7 K	40.3 $\pm$ 1.1 K
$U_{355K} - U_{295K}$	53.6 K $\pm$ 0.57 K	52.7 K $\pm$ 1.1 K

1 shows the mean temperature of the phantom voxels as well as their standard deviation. Looking at Tab 1. clarifies that using the Kaczmarz algorithm results in a more noisy and inaccurate temperature reconstructions, while the reconstruction with CGNR is less noisy as shown by the lower standard deviation of the mean of the five voxels. However, to achieve precise temperatures using the multi-color approach and the given data, further evaluation of the frequency selection as well as the choice of regularizing parameters  $\lambda$  and the number of iterations is required.

### III.III. Using a difference system matrix

Another approach of reconstructing temperatures is by using the difference of system matrices  $S_{\text{diff}} = [S_{335K} - S_{295K}]$  which is used to reconstruct the difference of the signal  $U_{\text{diff}} = U_T - U_{295K}$ . Again, the reconstruction is performed using Kaz and CGNR with 5 iterations and  $\lambda = 0.1$ . While the multi-color approach with CGNR required 50 iterations to converge, in this case 5 iterations are sufficient using the given data. Fig. 4 shows the reconstructed temperature differences for three different spectra  $U_{\text{diff}}$ , where  $U_{\text{diff}}$  is set to  $(U_{315K} - U_{295K})$ ,  $(U_{335K} - U_{295K})$  and  $(U_{355K} - U_{295K})$ . Fig. 4 top shows the reconstructed temperatures using CGNR and Fig. 4 bottom the reconstructions with the Kaczmarz method. The temperature is obtained by multiplying the reconstruction with the temperature difference between the system matrices in  $S_{\text{diff}}$  which is  $\Delta T = 40\text{K}$ . In addition, the temperatures are normalized by the particle concentration. As in section III.II, it is assumed that the particle signal is linear proportional to the temperature in the given range (295 K – 355 K). Tab. 2 shows the reconstructed temperature (mean) values with the corresponding standard deviation. It is visible that the CGNR method provides a slightly smoother reconstruction in this case. The reconstructed temperatures match good with the temperature difference within the difference measurements  $\mathbf{U}_{\text{diff}}$ . Nevertheless, the re-

constructed measurement  $\mathbf{U}_{335K} - \mathbf{U}_{295K}$  reconstructs to a temperature difference of approximately 50 K instead of 60 K. This may occur because the linearity assumption does not hold, the chosen frequency selection is suboptimal for the measurement at 355 K or because 355 K is an extrapolation outside of the range covered by the system matrices (295 and 335 K). Further investigations are necessary to understand this behaviour.

## IV. Conclusions

The development of precise methods for temperature reconstruction in MPI requires data in the form of system matrices and phantom/image measurements. This data must be reliable to be able to evaluate the methods at precisely known temperatures. In the case of experimental acquired data, this can be quite challenging. Therefore, using simulated data to generate system matrices and measurements has great potential as it can provide data with perfectly controllable parameters. This enables options to improve and develop methods as mentioned above in fields like MPI or MPH. In this work, the simulation-based data is used to examine methods to reconstruct temperature differences. The acquired results in particularly for the multi-color approach are not yet satisfactory, while for the second approach the reconstructed temperatures are approximately correct. The main issues to get reliable temperature accuracies in the range below  $\Delta T = 1$  K is to have a frequency selection fitting for every measurement at a given temperature. It is also shown, how the selected reconstruction method influences the reconstructed temperature image and that different methods show quite different results. Therefore, further investigations of the reconstruction behaviour at different temperatures are necessary. In addition, the linearity assumption (increasing signal versus increasing temperature) must be examined in dependence of

particle parameters such as magnetic anisotropy energy  $K_u$ ,  $V_M$  or hydrodynamic radius to understand its role in the reconstruction method.

## Author's statement

Conflict of interest: Authors state no conflict of interest.

## References

- [1] Jordan et al., Magnetic fluid hyperthermia (MFH): Cancer treatment with AC magnetic field induced excitation of biocompatible superparamagnetic nanoparticle, *Journal of Magnetism and Magnetic materials* 1-3, vol. 201, pp. 413-419, 1999
- [2] Duty et al., Magnetic particle hyperthermia – a promising tumour therapy?, *Nanotechnology* 45, vol. 25, pp. 452001, 2014
- [3] Haar et al., High intensity focused ultrasound-a surgical technique for the treatment of discrete liver tumours, *Physics in Medicine & Biology* 11, vol. 34, pp. 1743, 1989
- [4] J. Overgaard, Effect of hyperthermia on malignant cells in vivo: A review of hypotheses, *Cancer* 6, Vol. 39, pp. 2637, 1977
- [5] Weaver et al., Magnetic nanoparticle temperature estimation, *Medical Physics* 5, vol. 36, pp. 1822-1829, 2009
- [6] Stehning et al., Simultaneous magnetic particle imaging (MPI) and temperature mapping using multi-color MPI, *IJMPI* 2, 1612001, 2016
- [7] Salamon et al., Visualization of spatial and temporal temperature distributions with magnetic particle imaging for liver tumor ablation therapy, *Scientific reports* 1, vol. 10, pp. 1-11, 2020
- [8] Neumann et al., Stochastic simulations of magnetic particles: Comparison of different methods, *IWMPI*, pp. 213, 2018
- [9] <https://github.com/Neumann-A/StochasticPhysics>
- [10] Klemme et al. Exploring Parameters of Magnetic Particles in 1D Field Excitation, *IJMPI* 2, 2004001, 2020
- [11] Wells et al., Temperature dependence in magnetic particle imaging, *AIP Advances* 5, vol. 8, pp. 056703, 2018
- [12] T. Knopp and T.M. Buzug, *Magnetic particle imaging: an introduction to imaging principles and scanner instrumentation*, Springer Science, 2012